

# A rational complexing-reduction route to antimony nanotubes

Hanmei Hu,<sup>b</sup> Maosong Mo,<sup>b</sup> Baojun Yang,<sup>b</sup> Mingwang Shao,<sup>b</sup> Shuyuan Zhang,<sup>a</sup> Qiaowei Li<sup>b</sup> and Yitai Qian<sup>\*ab</sup>

<sup>a</sup> Structure Research Laboratory, University of Science and Technology of China, Hefei, Anhui 230026, P. R. China

<sup>b</sup> Department of Chemistry, University of Science and Technology of China, Hefei, Anhui 230026, P. R. China. E-mail: yitaiqian@ustc.edu.cn; Fax: +86 551 363 1760

Received (in Montpellier, France) 2nd April 2003, Accepted 4th June 2003

First published as an Advance Article on the web 2nd July 2003

**Antimony nanotubes with inner diameters of 15–80 nm, wall thickness of 10–30 nm and lengths of up to several micrometers have been successfully prepared by a rational complexing-reduction route using zinc powder as reductant at low temperature (80–140 °C).**

Since the discovery of carbon nanotubes,<sup>1</sup> much attention has been focused on nanotube materials due to their novel properties and promising applications in nanodevices.<sup>2</sup> Many types of nanotubes such as MX<sub>2</sub> (M = Mo or W, X = S or Se),<sup>3</sup> BN,<sup>4</sup> NiCl,<sup>5</sup> vanadium oxide,<sup>6</sup> InS,<sup>7</sup> NbS<sub>2</sub> and TaS<sub>2</sub>,<sup>8</sup> Bi<sub>2</sub>S<sub>3</sub>,<sup>9</sup> and organic nanotubes<sup>10</sup> have been reported. There has been a steadily increasing interest in the study of metallic nanotubes in recent years. Generally, template-based techniques have been used to prepare metallic nanotubes such as Au,<sup>11</sup> Ni,<sup>12</sup> Fe and Co.<sup>13</sup> Metallic Bi nanotubes have been prepared by a controlled hydrothermal reduction method, which suggests that the formation of Bi nanotubes may be associated with its layered structure.<sup>14</sup> Similar to the α-Bi structure, α-Sb also has a pseudolayered structure. In the same layer, each Sb atom is coordinated with three other Sb atoms by covalent bonds, thus forming a trigonal pyramid. These pyramids further form a puckered antimony layer with shared vertices. At the same time, each Sb atom contact three other Sb atoms in the adjacent layer *via* weak van der Waals forces. The above observations stimulated us to consider the possibility of preparing nanotubes of antimony with a layered structure.

Antimony is a semimetal whose energy overlap between the conduction and valence bands is about 180 meV at 4.2 K.<sup>15</sup> As in Bi, electronic transport phenomena in Sb occur *via* both electrons and holes. Amorphous or polycrystalline antimony nanowires have been prepared in porous anodic alumina templates using the vapor phase deposition technique and their particular transport properties have been also studied.<sup>16–18</sup> Recently, single-crystalline antimony nanowire arrays have been prepared by pulsed electrodeposition in anodic alumina membranes.<sup>19</sup> However, studies of the rational synthesis, physical properties and potential application of antimony nanotubes are still a challenge for chemical and material science researchers.

Herein, a rational complexing-reduction route was developed to synthesize Sb nanotubes under controlled solvothermal conditions. In our synthetic system, acetylacetone was selected as both solvent and complexing agent. Antimony chloride, taken as the antimony source, was coordinated with acetylacetone to form Sb-acetylacetone complexes, which were then reduced *in situ* to antimony products by zinc powder under certain conditions. The pH value of the reaction system is 1–2 before the reductive reaction takes place, while the pH

value is about 5 after completion of the chemical reaction. Hence, a possible chemical reaction pathway may be described as follows:<sup>20</sup>

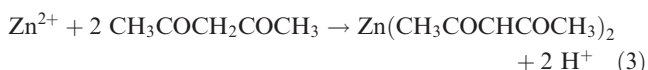
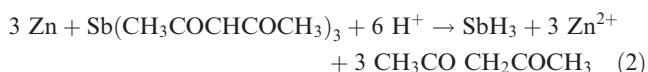
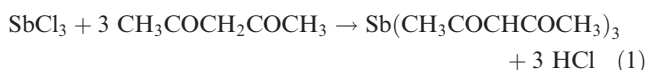


Fig. 1 shows a typical XRD pattern of the as-synthesized antimony products. All of the strong and sharp reflection peaks can be readily indexed to a pure rhombohedral lattice structure of antimony with calculated lattice constants  $a = 4.286 \text{ \AA}$  and  $c = 11.256 \text{ \AA}$ , which is in agreement with the literature values of  $a = 4.307 \text{ \AA}$  and  $c = 11.27 \text{ \AA}$  (JCPDS 05-0562). No impurity peaks were detected. Energy-dispersive X-ray (EDX) analysis of the nanotubes indicates that they are pure antimony (Fig. 2).

On the basis of TEM observations, the yield of Sb nanotubes is *ca.* 50%. Figs. 3(a) and 3(b) show the tubular morphologies of the as-prepared Sb products. They have inner diameters of 15–80 nm, wall thickness of 10–30 nm and lengths of up to several micrometers with obvious open ends. Most of the nanotubes are flexible and tend to bend. Fig. 3(c) shows a typical bent nanotube. One Sb nanotube was characterized by its SAED pattern [inserted in Fig. 3(b)]. Diffuse diffraction spots are due to the cylindrical structure of the sample. The HRTEM image of an individual Sb nanotube, shown in Fig. 3(e), unambiguously reveals the multiwalled structure. The average distance between the neighboring fringes is *ca.* 3.107 Å,

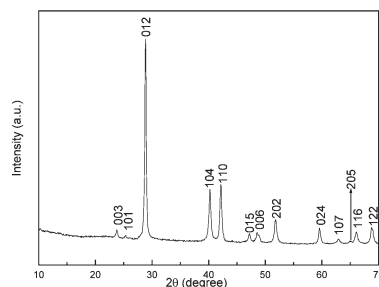


Fig. 1 XRD pattern of the as-synthesized antimony products.

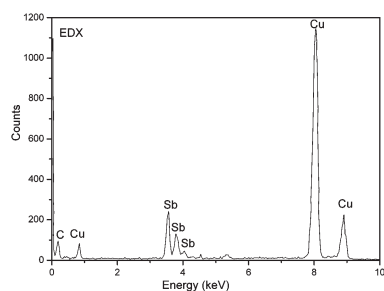


Fig. 2 EDX spectrum of an individual antimony nanotube.

corresponding to the (012) plane lattice distance in rhombohedral antimony. Moreover, the Sb nanotubes always coexist with sheets and structures with an unfinished tube-like morphology [indicated by the arrow in Fig. 3(d)]. The observed rolling phenomenon suggests that the formation of Sb nanotubes really has a close relation with its pseudolayered structure. Similar results have been previously reported in the preparation of  $\text{WS}_2$  nanotubes and a “rolling mechanism” was proposed.<sup>21</sup> Remskkar and coworkers have obtained direct evidence for the derivation of  $\text{MoS}_2$  tubules from the bending of platelets.<sup>22</sup> Li suggested a rolling of layered structures to achieve Bi nanotubes and proposed a 3-D model for Bi nanotubes.<sup>14</sup> Here, our experimental results also suggest that the formation of Sb nanotubes may be the result of the rolling of the layered structure. Further study of its mechanism is in progress.

Surely, the layer structure of antimony is indispensable for the formation of its nanotubes. And yet, the solvothermal treatment should provide a possible driving force for the nucleation and growth of antimony nanotubes. We speculate that the acetylacetone solvent not only may act as a complexing agent but also may play the same role as amines,<sup>23</sup> which act as a structure-directing agent for the growth of Sb nanotubes. Acetylacetone is a bidentate ligand with two anchor

oxygen atoms, which can complex with almost every metal in the periodic table to form coordination complexes.<sup>24</sup> When anhydrous  $\text{SbCl}_3$  was added to acetylacetone, the solution gradually turned from colorless to yellow at room temperature, which implies that Sb-acetylacetone complexes might be formed in the solution. Fig. 4 shows the IR spectra of pure acetylacetone and of an acetylacetone solution containing  $\text{Sb}^{3+}$  ions, respectively. In spectrum a, the two absorption bands at 1729 and 1710  $\text{cm}^{-1}$  can be assigned to the normal carbonyl frequencies. The broad band at 1622  $\text{cm}^{-1}$  is due to the conjugated, hydrogen-bonded carbonyl group characteristic of the enolic form of the  $\beta$ -diketone.<sup>25</sup> Although there are some disturbances of the free solvent molecules in spectrum b, some differences are apparent between spectra a and b. In spectrum b, the absorption bands at 1606 and 1558  $\text{cm}^{-1}$  can be assigned to chelated carbonyl and the C=C stretch, respectively.<sup>25</sup> The two bands at 1721 and 1685  $\text{cm}^{-1}$  may result from the cooperation of free solvent molecule and chelated carbonyl. The lowering of the carbonyl frequency can be attributed to acetylacetone coordinating with metal to form the coordination complexes. Production of the complexes could reduce the concentration of free  $\text{Sb}^{3+}$  ions in solutions, making the reaction mainly proceed *in situ* at the complexes and providing enough time and opportunity for the growth of Sb nanotubes. Moreover, the adsorption of the solvent to specific surfaces of the crystals may also affect the morphology of the final product.

Although we cannot yet put forward a reliable model for the structure of the Sb-acetylacetone complexes, the present experimental results reveal that the complexes may be essential for the formation of Sb nanotubes. It is possible that the Sb-acetylacetone complexes serve as an intermediate or a molecular template in the control of the growth of Sb nanotubes. More in-depth studies are still needed to explore the effects of the complexing solvent on the growth processes of the antimony nanotubes.

The effects of the temperature and solvent on the morphology of the Sb products have been investigated. It was found that higher or lower temperatures are not favorable for the

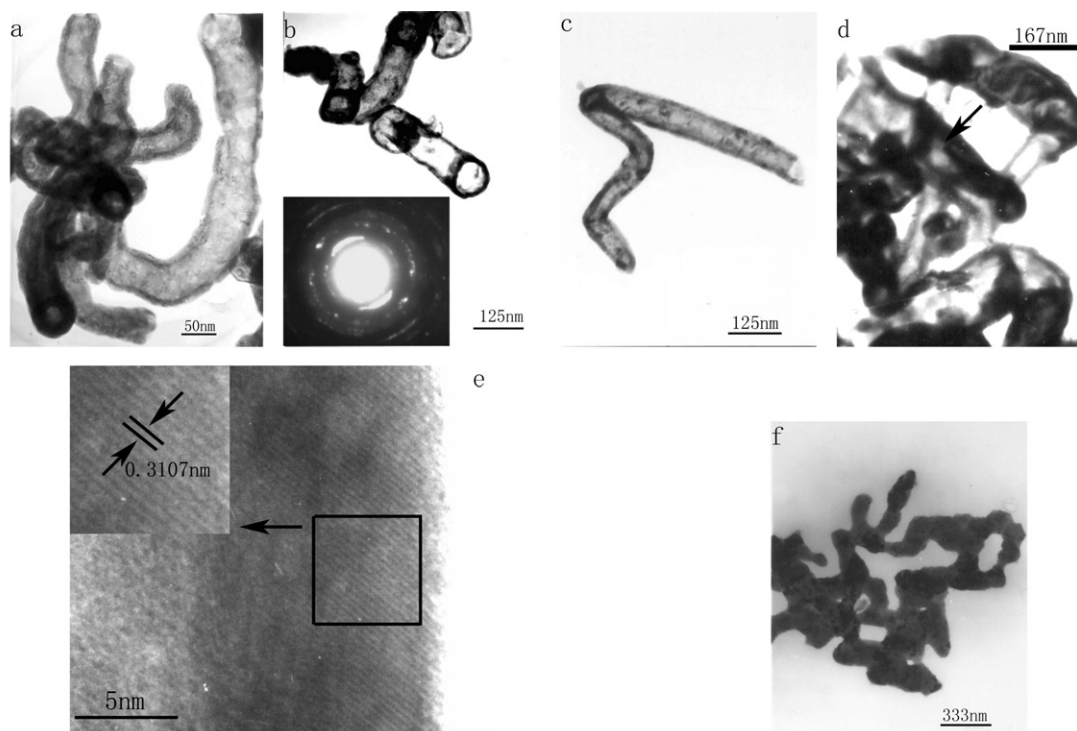


Fig. 3 TEM images showing (a) and (b) several Sb nanotubes, SAED pattern inserted in (b); (c) a typical bent nanotube; (d) the coexistence of well-defined nanotubes, unfinished tubular structures and sheets; (e) HRTEM image of the Sb nanotubes; (f) chain-like morphology obtained at 180 °C.

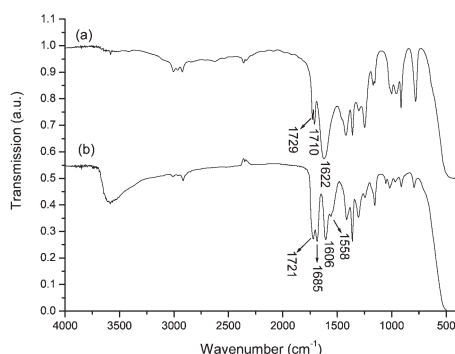


Fig. 4 IR spectra of (a) pure acetylacetone and (b)  $\text{Sb}^{3+}$ -containing acetylacetone solution.

formation of Sb nanotubes. For example, the products obtained at  $180^\circ\text{C}$  were not nanotubes or plates but chainlike networks with fractal feature [Fig. 3(f)], which were composed of nanoparticles. A possible reason is that higher temperature greatly decreases the stability of the Sb-acetylacetone complexes, quickens the release of  $\text{Sb}^{3+}$  from the complexes, allowing the reaction to occur not at the complexes but in the free solution and resulting in an extremely fast nucleation process and the production of many more nuclei. These newly produced particles tend to agglomerate with each other by self-organization, forming a chainlike pattern in order to lower their surface energy. No tubular structures were obtained using other solvents with different coordination abilities, such as ethanol, ethylene glycol, water and ethylenediamine. The present experiment suggests that acetylacetone may be the most appropriate solvent to fabricate Sb nanotubes and the appropriate reaction temperature should be in the range of  $80\text{--}140^\circ\text{C}$ .

In conclusion, a rational complexing-reduction route was developed to synthesize Sb nanotubes with inner diameters of  $15\text{--}80\text{ nm}$ , wall thickness of  $10\text{--}30\text{ nm}$  and lengths of up to several micrometers. The coexistence of tubular, unfinished tube-like and sheetlike structures in the as-synthesized antimony products indicates that the formation of antimony nanotubes may be associated with its layered structure. The acetylacetone solvent is thought to act as complexing agent, structure-directing agent and accelerator for the formation of antimony nanotubes. The obtained seamless antimony nanotubes with open ends may provide interesting possibilities for further studying their electronic properties, quantum effects and potential applications. The present work has enlarged the family of nanotubes and offers a possible method to synthesize nanotubes of other materials with analogous structure.

## Experimental

In a typical synthesis,  $0.456\text{ g}$   $\text{SbCl}_3$  and excess zinc powder ( $0.6\text{ g}$ ) were placed in a  $50\text{ mL}$  Teflon-lined stainless steel autoclave, which was then filled with acetylacetone up to 90% of the total volume. The sealed autoclave was maintained at  $\sim 100^\circ\text{C}$  for 12 h, then allowed to cool to room temperature naturally. The resulting solid products were filtered off, washed several times with absolute alcohol, dilute HCl and distilled water, and then finally dried in vacuum at  $60^\circ\text{C}$  for 6 h.

The X-ray powder diffraction (XRD) pattern was recorded using a Philips X'Pert PRO SUPER X-ray diffractometer with graphite monochromated  $\text{Cu-K}\alpha$  radiation ( $\lambda = 1.54187\text{ \AA}$ ). The morphologies of the prepared Sb products were characterized with a Hitachi model H-800 transmission electron microscope.

HRTEM images and EDX analysis were taken with a JEOL-2010 transmission electron microscope with an accelerating voltage of  $200\text{ kV}$ . FT-IR spectra were measured on a Bruker Vector-22 FT-IR spectrophotometer in the region of  $4000\text{--}400\text{ cm}^{-1}$ .

## Acknowledgements

Financial support from the National Natural Science Foundation of China and the 973 Projects of China is gratefully acknowledged.

## References

- 1 S. Iijima, *Nature (London)*, 1991, **354**, 56.
- 2 P. G. Collins, A. Zettl, H. Bando, A. Thess and R. E. Smalley, *Science*, 1997, **278**, 100.
- 3 (a) R. Tenne, L. Margulis, M. Genut and G. Hodes, *Nature (London)*, 1992, **360**, 444; (b) Y. Feldman, E. Wasserman, D. J. Srolovitz and R. Tenne, *Science*, 1995, **267**, 222; (c) R. Tenne, M. Homyonfer and Y. Feldman, *Chem. Mater.*, 1998, **10**, 3225.
- 4 N. G. Chopra, R. J. Luyken, K. Cherrey, V. H. Crespi, M. L. Cohen, S. G. Louie and A. Zettl, *Science*, 1995, **269**, 966.
- 5 Y. R. Hachohen, E. Grunbaum, R. Tenne, J. Sloan and J. L. Hutchison, *Nature (London)*, 1998, **395**, 336.
- 6 M. E. Spahr, P. Bitterli, R. Nesper, M. Müller, F. Krumeich and H. U. Nissen, *Angew. Chem., Int. Ed.*, 1998, **37**, 1263.
- 7 J. A. Hollingsworth, D. M. Poojary, A. Clearfield and W. E. Buhro, *J. Am. Chem. Soc.*, 2000, **122**, 3562.
- 8 M. Nath and C. N. R. Rao, *J. Am. Chem. Soc.*, 2001, **123**, 4841.
- 9 C. H. Ye, G. W. Meng, Z. Jiang, Y. H. Wang, G. Z. Wang and L. D. Zhang, *J. Am. Chem. Soc.*, 2002, **124**, 15180.
- 10 (a) M. R. Ghadiri, J. R. Granja, R. A. Milligan, D. E. Mcree and N. Khazanovich, *Nature (London)*, 1993, **366**, 324; (b) M. R. Ghadiri, J. R. Granja and L. K. Buehler, *Nature (London)*, 1994, **369**, 301.
- 11 (a) C. J. Brumlik and C. R. Martin, *J. Am. Chem. Soc.*, 1991, **113**, 3174; (b) C. R. Martin, M. Nishizawa, K. Jirage and M. Kang, *J. Phys. Chem. B*, 2001, **105**, 1925.
- 12 J. C. Bao, C. Y. Tie, Z. Xu, Q. F. Zhou, D. Shen and Q. Ma, *Adv. Mater.*, 2001, **13**, 1631.
- 13 G. Tourillon, L. Pontonnier, J. P. Levy and V. Langlais, *Electrochem. Solid. State. Lett.*, 2000, **3**, 20.
- 14 Y. D. Li, J. W. Wang, Zh. X. Deng, Y. Y. Wu, X. M. Sun, D. P. Yu and P. D. Yang, *J. Am. Chem. Soc.*, 2001, **123**, 9904.
- 15 L. R. Windmiller, *Phys. Rev.*, 1966, **149**, 472.
- 16 J. Heremans, C. M. Thrush, Y. M. Lin, S. Cronin, Z. Zhang, M. S. Dresselhaus and J. F. Mansfield, *Phys. Rev. B*, 2000, **61**, 2921.
- 17 J. Heremans, C. M. Thrush, Y. M. Lin, S. B. Cronin and M. S. Dresselhaus, *Phys. Rev. B*, 2001, **63**, 85406.
- 18 M. Barati, J. C. L. Chow, P. K. Ummat and W. R. Datars, *J. Phys. Condens. Matter.*, 2001, **13**, 2955.
- 19 Y. Zhang, G. H. Li, Y. Ch. Wu, B. Zhang, W. H. Song and L. D. Zhang, *Adv. Mater.*, 2002, **14**, 1227.
- 20 S. C. Chen, *Important Inorganic Chemical Reaction*, 2nd edn., Scientific Technology Press, Shanghai, 1982, p. 162.
- 21 Y. D. Li, X. L. Li, R. R. He, J. Zhu and Z. X. Deng, *J. Am. Chem. Soc.*, 2002, **124**, 1411.
- 22 M. Remskar, Z. Skraba, F. Cléton, R. Sanjinés and F. Lévy, *Appl. Phys. Lett.*, 1996, **69**, 351.
- 23 X. Chen, X. M. Sun and Y. D. Li, *Inorg. Chem.*, 2002, **41**, 4524.
- 24 (a) A. Camerman, D. Mastropaolo and N. Camerman, *J. Am. Chem. Soc.*, 1983, **105**, 1584; (b) F. Hirota and S. Shibata, *J. Mol. Struct. (THEOCHEM)*, 1986, **30**, 373; (c) R. Singhai, S. N. Limage and M. C. Saxena, *J. Ind. Chem. Soc.*, 1997, **74**, 633; (d) L. Broussous, C. V. Santilli and S. H. Pulcinelli, *J. Phys. Chem. B*, 2002, **106**, 2855.
- 25 (a) R. L. Belford, A. E. Martell and M. Calvin, *J. Inorg. Nucl. Chem.*, 1956, **2**, 11; (b) J. P. Dismukes, L. H. Jones and John C. Bailar, Jr., *J. Phys. Chem.*, 1961, **65**, 792.